Clinical Radiology 78 (2023) 509–517

Contents lists available at ScienceDirect

Clinical Radiology

journal homepage: www.clinicalradiologyonline.net

Review

Neuroimaging findings in paediatric patients with sickle cell disease

V. Sousa Abreu [a,*], S. Xavier [b], M. Santos [b], R. Lopes da Silva [c], P. Kjöllerström [d], C. Conceição [e]

[a] Neuroradiology Department, Centro Hospitalar Universitário do Porto, Porto, Portugal
[b] Neuroradiology Department, Hospital de Braga, Braga, Portugal
[c] Paediatric Neurology Unit, Hospital Dona Estefânia, Centro Hospitalar Universitário Lisboa Central, Lisboa, Portugal
[d] Paediatric Hematology Unit, Hospital Dona Estefânia, Centro Hospitalar Universitário Lisboa Central, Lisboa, Portugal
[e] Neuroradiology Department, Centro Hospitalar Universitário Lisboa Central, Lisboa, Portugal

ARTICLE INFORMATION

Article history:
Received 31 December 2022
Received in revised form
15 February 2023
Accepted 16 February 2023

Sickle cell disease (SCD) is an autosomal recessive haemoglobinopathy, which manifests as multisystem ischaemia and infarction, as well as haemolytic anaemia. The morphological changes of red blood cells (RBCs) that promote ischaemia/infarction as the main multisystemic manifestation, with associated vasculopathy, may also lead to haemorrhage and fat embolisation. Bone infarctions, whether of the skull or spine, are relatively common with subsequent increased infectious susceptibility. We present a broad spectrum of brain and spine imaging findings of SCD from a level III paediatric hospital in Lisbon, between 2010 and 2022. Our aim is to highlight brain and spine imaging findings from a serial review of multiple patients with SCD and respective neuroimaging characterisation.

Introduction

Sickle cell disease (SCD) is the most common genetic haemoglobinopathy, characterised by a mutation within the β-globin chain of haemoglobin, causing an important structural molecular change (HbS).[1] In its deoxygenated form, the altered haemoglobin has a greater tendency to aggregate and contribute to the development of precipitating insoluble crystals leading to rigid deformation of red blood cells (RBCs) with a characteristic sickle shape. The altered shape and rigidity of the RBCs result in greater difficulty passing through narrow capillaries, which in turn contributes to RBC dysfunction, vascular congestion, haemolytic anaemia, and multisystem ischaemia/infarction.[1,2]

Familiarity with imaging findings of brain and spinal complications of SCD may prompt the diagnosis, prognostic stratification, and promote early therapeutic measures to protect against end-organ damage. The aim of the present review is to highlight neuroimaging findings of SCD, within the broad spectrum of its manifestations and complications, from a serial review of multiple patients from a tertiary hospital.

* Guarantor and correspondent: V. Sousa Abreu, Centro Hospitalar Universitário do Porto, Largo do Prof. Abel Salazar, 4099-001 Porto, Portugal. Tel.: +351253419472.
E-mail address: vrlsa1993@gmail.com (V.S. Abreu).

https://doi.org/10.1016/j.crad.2023.02.013
0009-9260/

Intracranial manifestations

Chronic anaemia

As the name implies, there is a state of chronic anaemia. The spontaneous density of blood in intracranial vessels is determined by the fraction of viable haemoglobin, with a linear relationship between the vessel's radiodensity and the haematocrit.[3] Although not specific, these patients may have a decrease in the spontaneous density of intracranial vessels, which in more severe cases may become quite noticeable on computed tomography (CT; Fig 1).

Ischaemic stroke

Ischaemic stroke is one of the most common and potentially devastating clinical manifestations, contributing to increased morbidity and mortality. In fact, after congenital cardiac malformations, SCD is the most common cause of paediatric ischaemic stroke, with a higher incidence in the first 10 years of life.[4,5] The risk is multifactorial and may be related to changes in the microvasculature, due to vascular congestion and endothelial dysfunction conditioned by abnormal RBC, and/or because of macrovascular disease, related to large arteries vasculopathy (see below), with potential cerebral thromboembolic complications.

Although any cerebral arterial territory may be affected, watershed territories including the frontal and parietal cortical/subcortical regions are mostly involved (Fig 2; Electronic Supplementary Material Figs. S1 and S2). The clinical presentation will always vary according to the extent and arterial territories involved, as well as the underlying pathophysiological mechanism (acute neurological deficit in cases of cerebral embolism, or alternatively, deficits of progressive installation if a local thrombotic mechanism prevails); however, most patients may be asymptomatic, particularly when vascular burden is restricted only to small subcortical white matter lesions in the watershed territories.

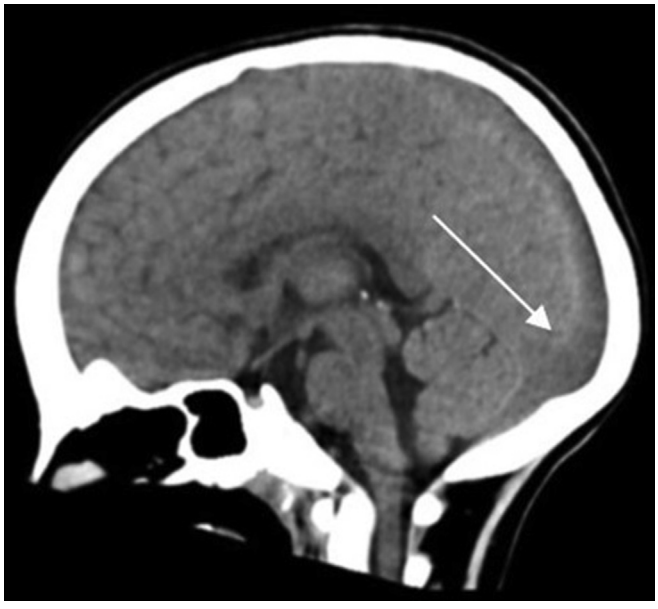

Figure 1 CT image of a 4-year-old male patient, with sagittal reconstruction showing marked hypodensity of the superior sagittal dural sinus (arrow), which becomes particularly evident when comparing with the normal cerebral parenchyma.

Regarding imaging, although it has lower sensitivity, CT may show areas of hyperacute/acute infarction with low density in the affected regions, and loss of grey–white matter differentiation (Electronic Supplementary Material Fig. S3); cerebral oedema/sulcal effacement or acute hyperdense intraluminal thrombus may be seen. On the other hand, magnetic resonance imaging (MRI) diffusion-weighted imaging (DWI) allows its detection in the first 30 minutes to 6 h,[6] with great sensitivity (Fig 2 and Electronic Supplementary Material Fig. S1), while conventional sequences (T1-and T2-weighted imaging) may not contribute during this period.[6] Stroke lesions will progress to chronicity, with gliotic and clastic areas, characterised by reduced volume, low density on CT, and high signal on long TR sequences at MRI (Electronic Supplementary Material Fig. S2 and S4).

Intracranial haemorrhage

Mainly due to micro- and macrovascular dysfunction, these patients also have an increased risk of intracranial haemorrhage, which may be intraparenchymal or extra-axial.[5] Although less common than ischaemic stroke, it appears more frequently during the second/third decade of life and is associated with higher mortality[5,7]

The most common cause is aneurysmal rupture, the incidence of which is higher in SCD patients, probably due to increased vessel fragility.[5] They also have a higher incidence of multiple aneurysms and higher risk of individual rupture. The vessel most frequently affected is the internal carotid artery (ICA), followed by the posterior cerebral arteries (PCA).[8]

Generally speaking, CT is particularly sensitive in detecting acute and subacute haemorrhagic lesions (Fig 3 and Electronic Supplementary Material Fig. S6), either in the intra- or extra-axial compartment, due to their spontaneously high density; however, among SCD patients, due to the chronic anaemia, blood products may present with lower density even in the acute phases, thus justifying the lower sensitivity of CT in these cases compared to MRI.[7] MRI is useful in its detection (Electronic Supplementary Material Fig. S5 and S6), depending on the phase of haemoglobin metabolism. Signal intensity will vary over time on T1-and T2-weighted images, the description of which is beyond the scope of this article, and it can be found elsewhere.[9] MRI susceptibility sequences, gradient echo (GRE) or susceptibility-weighted imaging (SWI; Electronic Supplementary Material Fig. S5), have higher sensitivity, allowing diagnosis of small lesions or, when already in a chronic phase (marked low signal due to the T2* effects of haemosiderin), which may be undetectable in conventional sequences.[9]

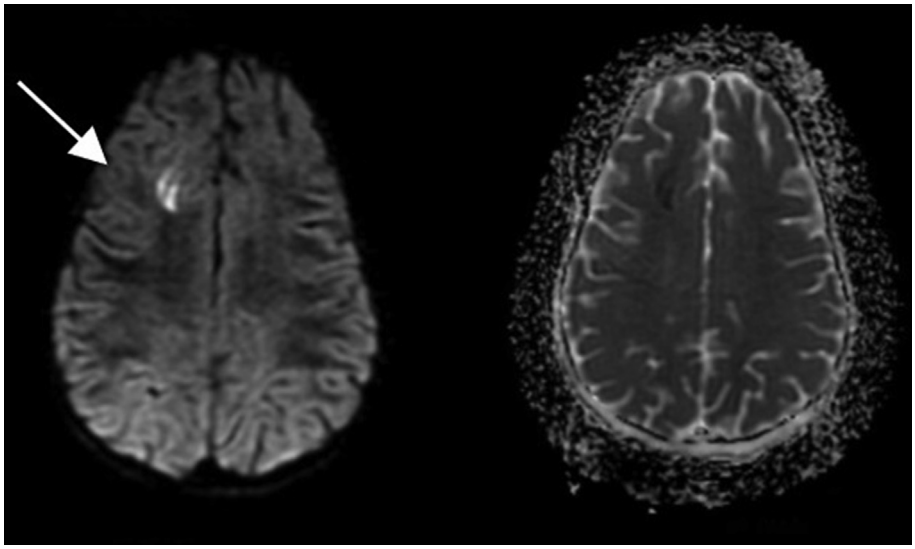

Figure 2 Axial MRI-DWI image (left) and corresponding ADC map (right) of a 3-year-old infant with SCD revealing focal high intensity lesions on DWI, and corresponding low signal on the ADC map, due to acute ischaemic lesions affecting the right frontal watershed arterial territory.

Figure 3 Axial CT image showing left lobar posterior temporal acute haemorrhage in a 16-year-old patient with SCD. The hyperdense oval haemorrhagic lesion is quite easy to see, surrounded by hypodense vasogenic oedema.

Intra- and extracranial vasculopathy

The presence of aberrant haemodynamics due to non-laminar flow in the intracranial large arteries, with subsequent endothelial damage is proposed as the main cause of the higher incidence of intracranial large-vessel vasculopathy in SCD.[10] It is mainly characterised by significant ectasia and tortuosity (Electronic Supplementary Material Fig. S7), most frequently affecting the intracranial ICAs, but also the vessels of the vertebrobasilar circulation. This involvement of the intracranial vasculature has already been well characterised in the Suzuki & Takaku staging system.[11] Although less common, it is well established that moyamoya vasculopathy involves more vessels than solely the intracranial ICA and MCA, as the extracranial carotid and vertebral arteries may also be dysmorphic in SCD patients (Fig 4).[12] In fact, due to this extracranial involvement, which surpasses the Suzuki classification, there have been alternative scoring systems in some SCD clinical trials using the number and severity of vessel involvement in determining treatment plans.[13,14]

All children and young adults diagnosed or with a clinical suspicion of SCD, particularly when asymptomatic, should be offered annual monitoring of the intracranial vasculature by transcranial Doppler ultrasound (TCD).[15,16] This is justified by the known association between high blood velocity in the cerebral arteries (reflecting steno-occlusive arterial vasculopathy) and the risk of a stroke.[15] The measured highest time averaged maximum mean velocity (TAMMV) prompt risk stratification: patients are at low risk with normal velocities ($<$170 cm/s), conditional risk with borderline velocities (between 170 and 199 cm/s), and at high risk when increased (ICA/MCA/ACA $\geq$200 cm/s).[16,17] On the other hand, low velocities ($<$70 cm/s in MCA) or pronounced asymmetry ($<$50% of contralateral MCA) should also alert to the possibility of arterial occlusion and should promote further investigation.[16]

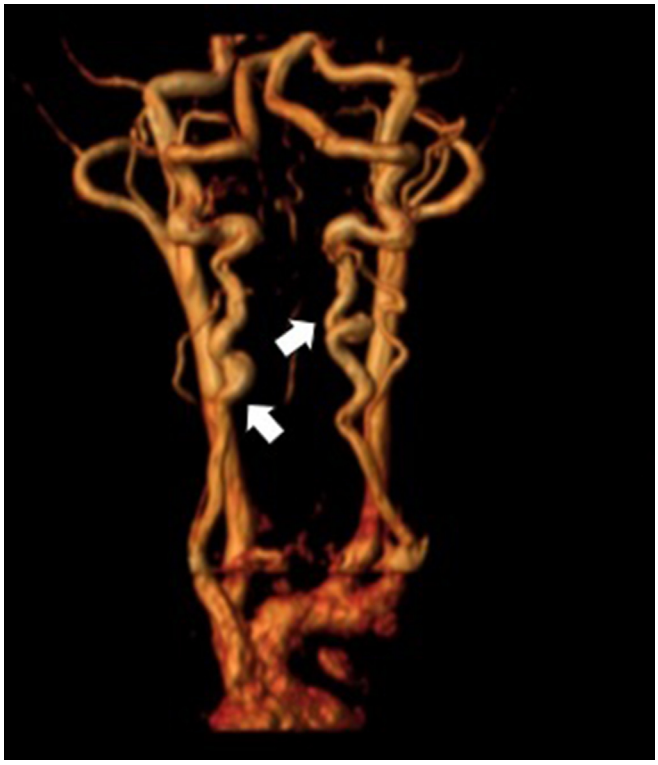

Figure 4 CTA three-dimensional maximum intensity projection reconstruction of an 8-year-old child. There is marked extracranial carotid and vertebral arterial tortuosity, particularly involving the vertebral arteries (open arrows), more severe on the left. In addition, note some irregularity of the partially covered intracranial vessels.

This assessment has a major impact on the guidance of these patients. If velocities are low or asymmetric, further imaging should be recommended, such as non-invasive angiographic study (CT angiography [CTA], MRI angiography [MRA]) or invasively (digital subtraction angiography [DSA]). TCD should be repeated when the risk is low (at 1 year) or conditional (at 6 weeks to 3 months). When the risk is considered high (Electronic Supplementary Material Fig. S8), it should be repeated in 1 week, and depending on the neurological assessment and the results of other imaging studies, transfusion treatment may be considered. It should be noted that once a child has started on regular transfusions, TCD surveillance must be maintained. Further understanding regarding TCD standards and guidance for children with SCD can be found at www.svtgbi.org.uk/media/resources/tcdstandards.pdf.

Conventional MRI, such as T2-wweighted images, due its flow-void proprieties, may show abnormal large vessels, although dedicated angiograms (CTA, MRA, or DSA) are usually necessary for a better characterisation.

In more severe cases, vasculopathy of large intracranial vessels may present with a steno-occlusive pattern, with involvement of the distal portion of the ICA and proximal segment of the MCA, thus characterising the moyamoya phenomenon, also typically associated to SCD.[18] With the progressive pathological involvement of these arteries, there is a compensatory prominence of collateral branches, particularly lenticulo-striatum and thalamo-perforating ones, which confer the classic “puff of smoke” image (Electronic Supplementary Material Fig. S9).

Although an angiographic study is necessary for its diagnosis and characterisation, the high T2/fluid-attenuated inversion recovery (FLAIR) signal and contrast enhancement of the cortical sulci characterises the “ivy sign” (Fig 5 and Electronic Supplementary Material Fig. S10), an indirect stigma of the compensatory dilated pial vessels with slowed flow that is relatively specific for moyamoya syndrome.[19] This sign may also reflect areas of regional decreased cerebral vascular reserve and increased ischaemic risk of the parenchyma in the vicinity, meaning that in addition to its diagnostic role, it is also characterised by its value as a prognostic biomarker.[20]

Ischaemia is usually explained by haemodynamically mediated hypoperfusion; cerebral perfusion studies (CT perfusion or MRI perfusion-weighted imaging [PWI]) are particularly relevant because they enable the identification of abnormal hypoperfused cerebral tissue. The arterial border zones are particularly at higher risk (with increased time to peak [TTP] or mean transit time [MTT], and normal or increased cerebral blood volume [CBV]), associated with relative preservation of central regions, reflecting its

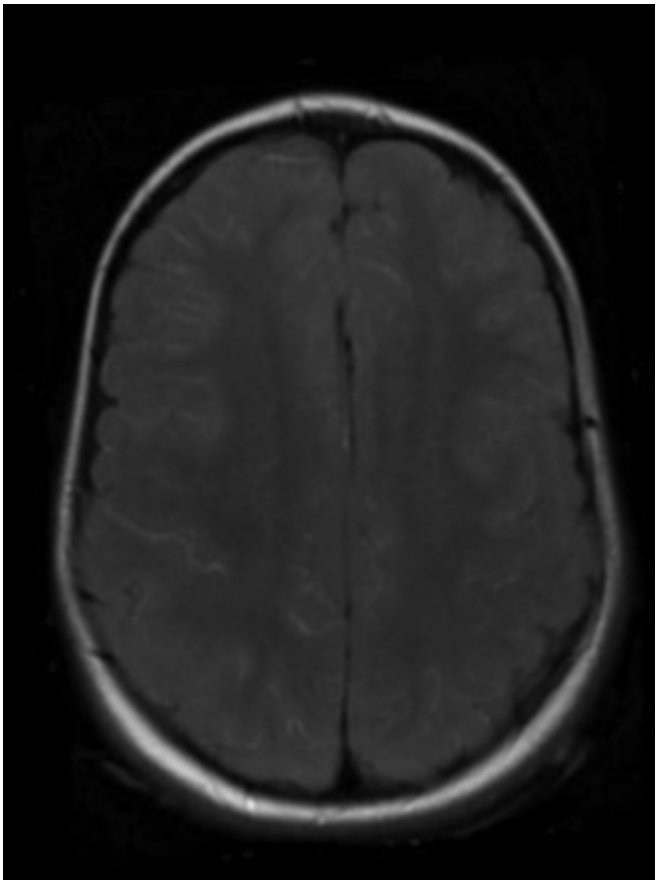

Figure 5 Axial T2/FLAIR image of a 16-year-old male patient with SCD, showing diffuse high signal of the cortical sulci (“ivy sign”), reflecting prominent pial vessels with slow flow, compensating for the steno-occluded proximal intracranial vessels.

characteristic proximal collateralisation pattern (Electronic Supplementary Material Figs. S10 and S11).[21,22] There is a demonstrated correlation between the degree of hypoperfusion (increased MTT) and the degree of intracranial steno-occlusive disease.[23] In addition to their importance in the diagnosis and stratification, perfusion studies may also be useful in assessing the response to treatment (medical but, above all, surgical) and follow-up (Electronic Supplementary Material Fig. S11).[24]

Surgery is generally recommended for the treatment of patients with recurrent or progressive cerebral ischaemic events and associated reduced cerebral perfusion reserve, particularly when the best medical treatment is insufficient.[25] The aim is to bypass the occlusive segments and this can be accomplished by direct (artery-to-artery anastomosis) or indirect revascularisation techniques.

External carotid artery to middle cerebral artery (ECA–MCA) or superficial temporal artery to middle cerebral artery (STA–MCA) direct anastomoses can be performed in adults as these vessels are larger[25]; however, indirect procedures are preferably chosen in the paediatric patients, and regardless of the technique, these rely on neovascularisation phenomenon. Within these, one can dissect the vascularised temporalis muscle and underlying galeal flap and lay them directly onto the pial surface of the brain (encephalomyosynangiosis), alternatively using the temporalis muscle, dura, and superficial temporal artery (encephaloduroarteriomyosynangiosis), or just the dura and superficial temporal artery (encephaloduroarteriosynangiosis).[25] Another surgical alternative is simply to create multiple burr holes to allow formation of local collaterals to the pial circulation (Electronic Supplementary Material Fig. S11).[26]

Cerebral perfusion imaging studies (particularly MRI-PWI) can be applied for evaluating postoperative changes in cerebral blood flow: shortening of the TTP or MTT in the MCA territory of the operated side should be considered as a marker for the development of collateral circulation (Electronic Supplementary Material Fig. S11).[24]

Fat embolisation syndrome

The multisystemic ischaemia that characterises SCD typically leads to multiple bone infarctions (see below) and bone marrow damage. This may lead to the release of fat globules as well as haematopoietic tissue into the systemic circulation via venous sinusoids within trabecular bone. Once they travel through the capillary beds, they can reach any organ through the venous system, with subsequent ischaemic microvascular injuries.[27,28] In addition to this microvascular occlusion mechanism, circulating phospholipids are metabolised and give rise to multiple inflammatory cytokines, which may also lead to endothelial damage, disruption of the blood–brain barrier, and ultimately microhaemorrhages.[28]

As the brain is no exception, it can also be a target for embolisation. MRI has a particularly important role in the diagnosis; these changes may be unnoticed on CT, particularly at an early stage. MRI-DWI may show multiple scattered punctate foci of cytotoxic oedema, reflecting small infarcted areas due to fat microemboli, leading to the so called “starfield sign”, resembling the starry night sky (Fig 6 and Electronic Supplementary Material Fig. S12).[29] Subcortical white matter diffuse microbleeds are easily visualised on magnetic susceptibility sequences (GRE or SWI),[30] typically presenting a “walnut kernel pattern” (Fig 7 and Electronic Supplementary Material Fig. S13).

Posterior reversible encephalopathic syndrome

Posterior reversible encephalopathy syndrome (PRES) is thought to be secondary to a self-regulatory inability of the vertebrobasilar circulation to respond adequately to sudden changes in systemic blood pressure (BP), and may be associated with several clinical entities, one of which is SCD[31]; however, BP changes are not responsible in all cases, and there are theories advocating a potential relationship with arterial vasospasm and/or endothelial dysfunction (a pathophysiological feature of SCD). It typically presents with altered consciousness, headaches, seizures, and visual changes.

Although the mechanism is debatable, it is generally accepted that blood–brain barrier dysfunction occurs with subsequent vasogenic oedema, represented by high T2/FLAIR

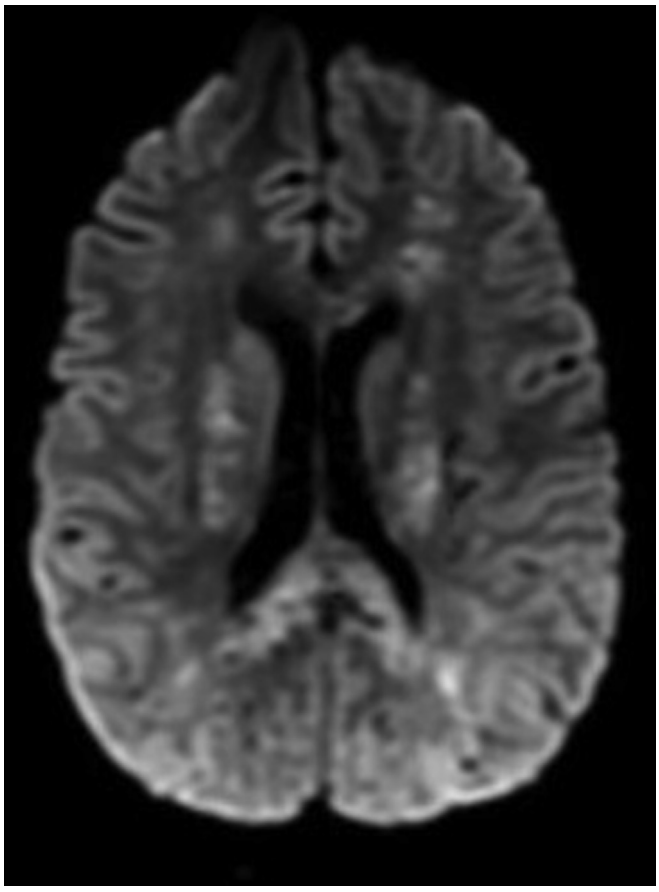

Figure 6 MRI-DWI axial image of a 17-year-old adolescent diagnosed with SCD, hospitalised due to respiratory distress, showing the typical “starfield pattern” of cerebral fat embolism syndrome with bilateral tiny DWI hyperintense foci within the white matter and grey matter, with some bias towards the watershed regions.

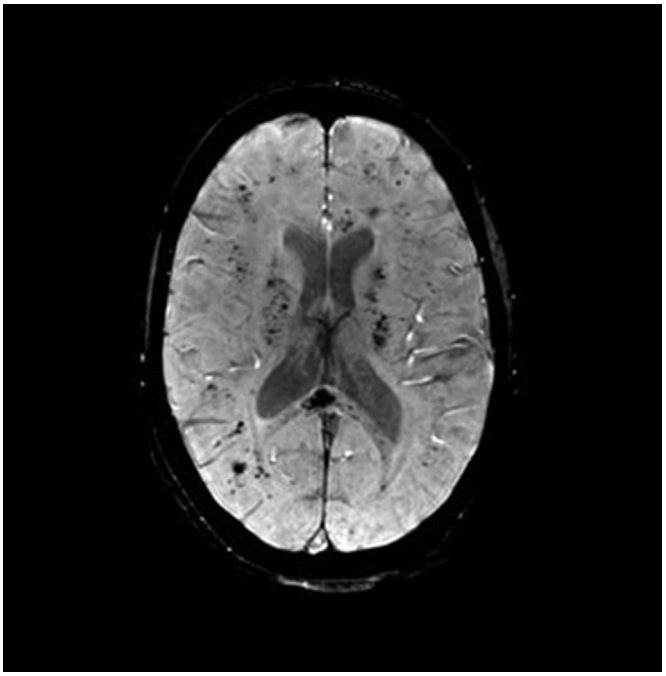

Figure 7 MRI-SWI of the same patient as Fig 6 showing multiple and profuse small foci of low intensity, essentially involving the white matter, representing microhaemorrhages due to fat embolisation ("walnut kernel pattern").

signal of the affected white matter, and associated mass effect.[32] Cytotoxic oedema may occur (high signal on DWI and low signal on ADC map), and although arguable, it possibly occurs due to mass effect from vasogenic oedema and subsequent microvasculature compression, or, alternatively, because of vasoconstriction/vasospasm and secondary low regional perfusion.[32,33] Classically, the involved areas are the parieto-occipital brain parenchyma, bilateral and symmetrically, although in a minority of cases it may occur in the watershed arterial territories (Electronic Supplementary Material Fig. S14), or even more rarely, in the basal ganglia or brainstem, unilaterally. Brain and sulcal haemorrhage may also occur in minor cases.[33] Compared to adults, PRES can manifest with more broad findings in childhood, with particularly higher propensity for haemorrhage (intra- and extra-axial), more frequent restricted diffusivity lesions, and more atypical patterns of parenchymal involvement.[34]

Bone manifestations

Skeletal involvement is particularly common in SCD and can be multifactorial, conditioned by chronic anaemia with subsequent extramedullary or excessive intramedullary haematopoiesis, vaso-occlusive crises leading to bone infarctions/osteonecrosis, or by infectious processes with osteomyelitis and related complications.[35]

Bone marrow hyperplasia

Excessive intramedullary haematopoiesis is characterised by excessive cell proliferation of the red marrow, affecting bone skeleton in a global way. Regarding the skull, there is enlargement of the diploic space and thickening of the bone trabeculae, giving rise to the "hair on end sign" in conventional radiology or CT.[35,36]

On MRI, these changes can be more easily detected, because in addition to bone expansion, there is also an important decrease in the normal T1 and T2 signal of the involved bone structures,[36] whether in the skull or spine (Electronic Supplementary Material Fig. S15); however, it must also be considered that the low signal on conventional sequences may also be partially explained in cases of SCD with iron overload from chronic RBC transfusion.

Finally, when there is quite severe anaemia, extramedullary haematopoiesis may occur, characterised by soft-tissue components surrounding the involved bone structures,[35,36] sometimes with increased risk for compressive cranial or peripheral neuropathies (when involving skull base or spine neural foramina, respectively) or for compressive myelopathy.

Bone ischaemia/osteonecrosis

Osteonecrosis due to ischaemic insults is one of the most frequent complications of SCD.[36] Bone infarcts in adults usually occur in locations with high bone marrow activity, such as the long bones or vertebrae. Maxillofacial bones and skull involvement is less common owing to the relatively small bone marrow cavity[37]; however, these structures may be involved during childhood as there is more diffuse haematopoietically active marrow. Typical facial bone infarcts affect the orbital walls or mandible,[38] and are clinically associated with regional pain and headache.[39]

CT is of limited use for diagnosis of acute marrow ischaemia and infarcts, despite being useful for identification of haemorrhagic or fluid associated collections (see below). Late subacute or chronic changes are also non-specific but easily detectable on CT, generally with reduced bone thickness and mixed osteosclerosis and osteolysis.[35,37]

MRI is useful in the detection of acute bone ischaemia and enables evaluation of marrow signal intensity changes. At an early stage, there is marrow oedema characterised by low T1 and high T2 signal (Electronic Supplementary Material Fig. S16), associated slight expansion, and heterogeneous or rim enhancement (correlating with the region of avascularisation).[37,39]

Spine vertebral involvement is the most common site for ischaemia and infarctions in these patients.[35] The same reasoning can be applied to spinal imaging presentation: acute disease is particularly difficult to diagnose using CT, with MRI being the most sensitive tool revealing bone marrow oedema (again, low T1, high T2 signal, slight expansion, and rim/heterogeneous enhancement; Electronic Supplementary Material Fig. S17). DWI may be particularly useful in diagnosing acute bone ischaemia and differentiating it from osteomyelitis, which may present with similar imaging and clinical findings; however, evolution of DWI/ACD signal intensity changes during an early ischaemic phase were recently described elsewhere[40] and

may be promising in distinguishing these two different entities (see below).

During late subacute and chronic stages, there may be reduced vertebral body height, chronically with areas of low T1 and T2 signal due to sclerosis and fibrosis, or T1 and T2 hyperintense foci due to fat degeneration.[35,36] At this stage, these changes are also easily detectable on CT (Fig 8 and Electronic Supplementary Material Fig. S18), which may show areas of sclerotic change in the subacute-to-chronic phase or radiolucency and cortical thinning/destruction, and progressive collapse of vertebral endplate, giving rise to typical "H-shaped" vertebrae (Electronic Supplementary Material Fig. S18 and S19).

Figure 8 CT image, sagittal reconstruction, bone window, of a patient with SCD, showing vertebral endplate depression, more severe in their central region, with consequent height reduction and vertebral bodies collapse, leading to the typical "H-shaped" morphology.

Extra-axial and extra-cranial collections

Non-traumatic extra-axial or epicranial collections, with fluid or associated haematic content, are a rare complication of SCD.[12,35,41] There are different pathophysiological mechanisms. Bone infarcts, or alternatively, multiple microfractures in a skull weakened by the diploe expansion and thinning of the inner and outer tables, can lead to blood, fluid, or proteinaceous material leakage into adjacent spaces. Finally, sludging RBCs in diploic veins may lead to venous congestion and consequent leakage.[41]

Depending on the nature of its content, there may be different radiodensities on CT: fluid–liquid collections are going to be hypodense, whereas large amounts of proteinaceous material may have higher densities. As for the haematic collections, their density will depend on their age, with recent ones being hyperdense, whereas chronic collections are usually hypodense; however, when SCD patients present with chronic severe anaemia (see above), these blood collections may have lower density even in the acute phase, due to the lower amount of normal haemoglobin (Fig 9 and Electronic Supplementary Material Fig. S20).[7,9]

On MRI, collections generally show a high T2 signal (remembering that T1 and T2 signal intensity will vary according to haemoglobin metabolism stage [Electronic Supplementary Material Fig. S21])[9]; either way, if haematic products are present, they are easily depicted on magnetic susceptibility sequences. T1, FLAIR, and DWI sequences can aid in extra-axial collection identification; the amount of protein is generally proportional to the signal on T1 and FLAIR images, while haematic or pyogenic content shows high signal on DWI, for example. Furthermore, MRI is particularly important in identifying potential bone infarctions, often underlying these collections.

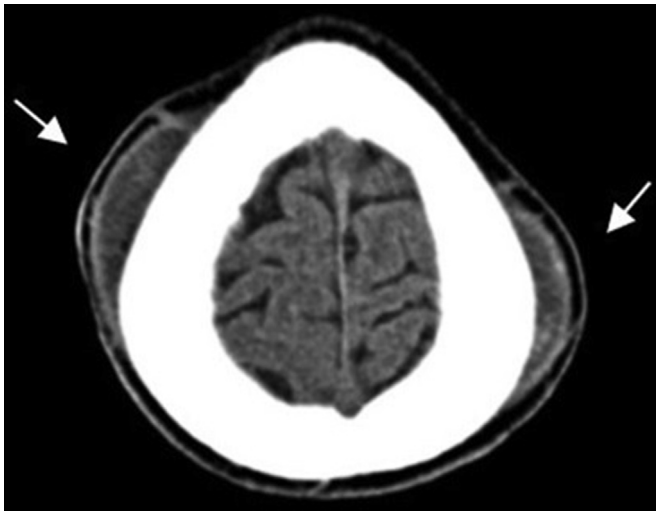

Figure 9 CT image of a 15-year-old male patient with SCD complaining of non-traumatic cranial bilateral swelling: axial images showing bilateral hypodense parietal epicranial collections (arrows) in a thickened skull. Due to severe chronic anaemia, blood collections in SCD patients, even in an acute phase, may present with low density.

Infectious complications

Due to functional asplenia and abnormal vascular flow, patients with SCD are at an increased risk of infection. Bone is particularly susceptible, mainly by haematogenous dissemination of *Salmonella* spp, followed by *Staphylococcus* spp.[35,42] Although bone infarction is a far more common event, its clinical presentation can be similar to osteomyelitis, and imaging distinction is also challenging.[35] During the early phase, both present with slight bone expansion and high T2 signal due to bone marrow oedema, and fluid collections may coexist (Fig 10 and Electronic Supplementary Material Fig. S22). Still, some imaging clues may help. While a blood collection favours a vascular mechanism, evidence of homogeneous restricted diffusion of its content points to infection, due to its pyogenic material.[35,43] The presence of an enhancing soft-tissue component associated in communication with the injured bone via some cortical defect favours osteomyelitis.[43] Moreover, the pattern of enhancement on post-gadolinium T1-weighted images may also help: while areas of early bone infarction may show peripheral ring enhancement, osteomyelitis is more often characterised by an irregular and geographic enhancing pattern of the infected bone marrow.[43] Finally, in cases of spine disease, the involvement of the intervertebral disc suggests an infectious aetiology.

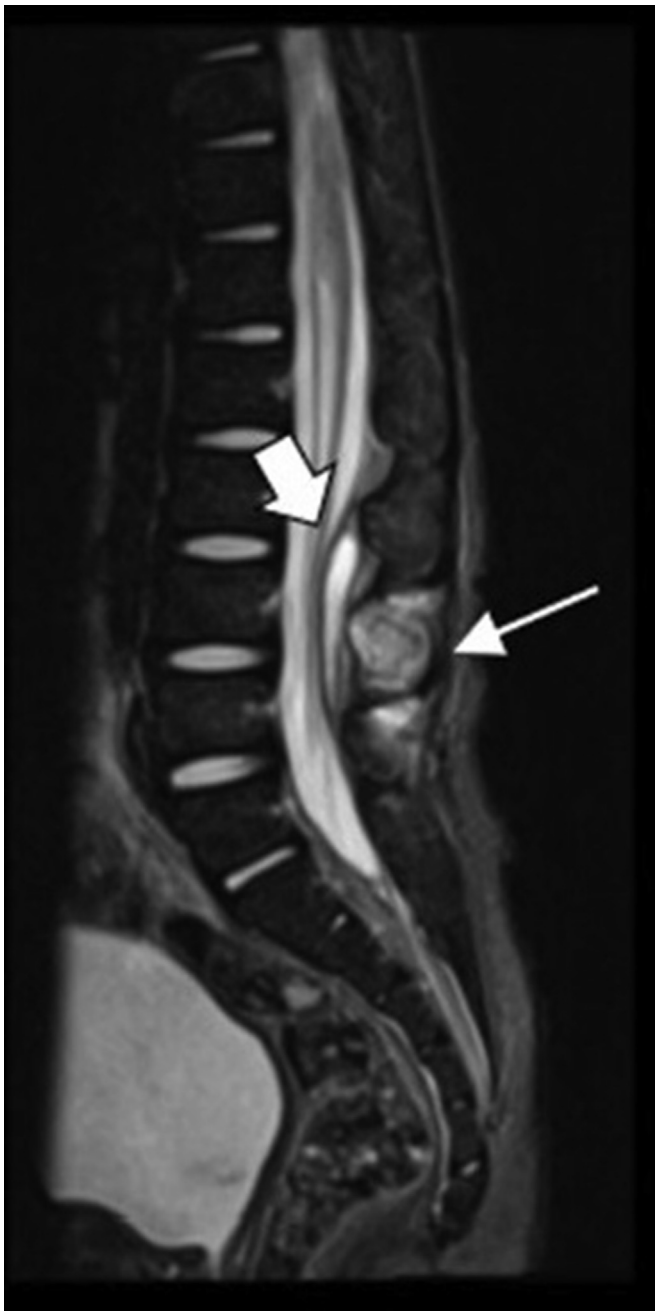

Figure 10 MRI of the lumbar spine, sagittal T2-weighted image of a young male patient with acute low back pain. There is high T2 signal of posterior vertebral elements at the low lumbar levels, with slight expansion (arrows) and associated epidural fluid collection (open arrow). Unfortunately, due to technical limitations, it was not possible to obtain post-gadolinium T1-weighted or DWI images, which would facilitate the diagnosis. Even though the patient had increased inflammatory parameters and fever, favouring osteomyelitis with associated epidural abscess/empyema, the patient underwent surgery and this diagnosis was confirmed.

Another recently described finding that may help is the evolution of the DWI/ADC signal at an early stage.[40] It is thought that due to the increased erythrocyte sickling and sequestration within the affected bone marrow (subsequent increased deoxyhaemoglobin), there is an early/hyperacute T2-blackout effect on DWI (low DWI and ADC signal), which can be associated with vaso-occlusive crisis. Later, once this phenomenon may lead to marrow infarction, there is subsequent bone restricted diffusion (DWI hyperintensity and ADC dark signal).

Conclusion

There are multiple manifestations and systemic complications of SCD, with important cranioencephalic and spinal involvement. Recognition of brain and spinal imaging findings, even the less commonly described, may prompt diagnosis and prognostic stratification, enabling the best therapeutic response, with the ultimate intent of improving patients' quality of life.

Conflict of interest

The authors declare no conflict of interest.

Appendix A. Supplementary data

Supplementary data to this article can be found online at https://doi.org/10.1016/j.crad.2023.02.013.

References

1. Kato GJ, Steinberg MH, Gladwin MT. Intravascular haemolysis and the pathophysiology of sickle cell disease. *J Clin Invest* 2017;**127**(3):750–60.
2. Bookchin RM, Lew VL. Pathophysiology of sickle cell anaemia. *Hematol Oncol Clin North Am* 1996;**10**(6):1241–53.

3. Ben Salem D, Osseby G, Rezaizadeh-Bourdariat K, *et al*. Vaisseaux intracrâniens spontanément hyperdenses au scanner en cas de polyglobulie. *J Radiol* 2003;**84**(5):605–8.
4. Mittal SO, ThatiGanganna S, Kuhns B, *et al*. Acute ischaemic stroke in paediatric patients. *Stroke* 2015;**46**(2).
5. Webb J, Kwiatkowski JL. Stroke in patients with sickle cell disease. *Expert Rev Hematol* 2013;**6**(3):301–16.
6. Srinivasan A, Goyal M, Al Azri F, *et al*. State-of-the-art imaging of acute stroke. *RadioGraphics* 2006;**26**(Suppl. 1):S75–95.
7. Kossorotoff M, Brousse V, Grevent D, *et al*. Cerebral haemorrhagic risk in children with sickle-cell disease. *Dev Med Child Neurol* 2015;**57**(2):187–93.
8. Yao Z, Li J, He M, *et al*. Intracranial aneurysm in patients with sickle cell disease: a systematic review. *World Neurosurg* 2017;**105**:302–13.
9. Bradley WG. MR appearance of haemorrhage in the brain. *Radiology* 1993;**189**(1):15–26.
10. Lonergan GJ, Cline DB, Abbondanzo SL. Sickle cell anaemia. *RadioGraphics* 2001;**21**(4):971–94.
11. Suzuki J. Cerebrovascular "moyamoya" disease. *Arch Neurol* 1969;**20**(3):288.
12. Buch K, Arya R, Shah B, *et al*. Quantitative analysis of extracranial arterial tortuosity in patients with sickle cell disease. *J Neuroimaging* 2017;**27**(4):421–7.
13. Ware RE, Davis BR, Schultz WH, *et al*. Hydroxycarbamide versus chronic transfusion for maintenance of transcranial Doppler flow velocities in children with sickle cell anaemia—TCD with Transfusions Changing to Hydroxyurea (TWiTCH): a multicentre, open-label, phase 3, non-inferiority trial. *Lancet* 2016;**387**(10019):661–70.
14. Helton KJ, Adams RJ, Kesler KL, *et al*. Magnetic resonance imaging/angiography and transcranial Doppler velocities in sickle cell anaemia: results from the SWiTCH trial. *Blood* 2014;**124**(6):891–8.
15. Adams RJ, McKie VC, Carl EM, *et al*. Long-term stroke risk in children with sickle cell disease screened with transcranial Doppler. *Ann Neurol* 1997;**42**(5):699–704.
16. Lee MT, Piomelli S, Granger S, *et al*. Stroke prevention trial in sickle cell anaemia (STOP): extended follow-up and final results. *Blood* 2006;**108**(3):847–52.
17. Kwiatkowski JL, Granger S, Brambilla DJ, *et al*. Elevated blood flow velocity in the anterior cerebral artery and stroke risk in sickle cell disease: extended analysis from the STOP trial. *Br J Haematol* 2006;**134**(3):333–9.
18. Kauv P, Gaudré N, Hodel J, *et al*. Characteristics of moyamoya syndrome in sickle-cell disease by magnetic resonance angiography: an adult-cohort study. *Front Neurol* 2019;**10**.
19. Mori N, Mugikura S, Higano S, *et al*. The leptomeningeal "ivy sign" on fluid-attenuated inversion recovery MR imaging in moyamoya disease: a sign of decreased cerebral vascular reserve? *AJNR Am J Neuroradiol* 2009;**30**(5):930–5.
20. Montaser AS, Lalgudi Srinivasan H, Staffa SJ, *et al*. Ivy sign: a diagnostic and prognostic biomarker for paediatric moyamoya. *J Neurosurg Paediatr* 2022;**29**(4):458–66.
21. Schubert GA, Czabanka M, Seiz M, *et al*. Perfusion characteristics of moyamoya disease. *Stroke* 2014;**45**(1):101–6.
22. Calamante F, Ganesan V, Kirkham FJ, *et al*. MR perfusion imaging in moyamoya syndrome. *Stroke* 2001;**32**(12):2810–6.
23. Togao O, Mihara F, Yoshiura T, *et al*. Cerebral haemodynamics in moyamoya disease: correlation between perfusion-weighted MR imaging and cerebral angiography. *AJNR Am J Neuroradiol* 2006;**27**(2):391–7.
24. Lee SK, Kim DI, Jeong EK, *et al*. Postoperative evaluation of moyamoya disease with perfusion-weighted MR imaging: initial experience. *AJNR Am J Neuroradiol* 2003;**24**(4):741–7.
25. Digiusto M, Bhalla T, Grondin R, *et al*. Perioperative care of the paediatric patient for pial synangiosis surgery. *Int J Clin Exp Med* 2013;**6**(3):231–8.
26. Symss N, Cugati G, Pande A, *et al*. Multiple burr hole surgery as a treatment modality for paediatric moyamoya disease. *J Paediatr Neurosci* 2010;**5**(2):115.
27. Tsitsikas DA, May JE, Gangaraju R, *et al*. Revisiting fat embolism in sickle syndromes: diagnostic and emergency therapeutic measures. *Br J Haematol* 2019;**186**(4).
28. Tsitsikas DA, Bristowe J, Abukar J. Fat embolism syndrome in sickle cell disease. *J Clin Med* 2020;**9**(11):3601.
29. Dhakal LP, Bourgeois K, Barrett KM, *et al*. The "starfield" pattern of cerebral fat embolism from bone marrow necrosis in sickle cell crisis. *Neurohospitalist* 2015;**5**(2):74–6.
30. Kuo KH, Pan YJ, Lai YJ, *et al*. Dynamic MR imaging patterns of cerebral fat embolism: a systematic review with illustrative cases. *AJNR Am J Neuroradiol* 2014;**35**(6):1052–7.
31. Frye RE. Reversible posterior leukoencephalopathy syndrome in sickle-cell anaemia. *Paediatr Neurol* 2009;**40**(4):298–301.
32. Tetsuka S, Ogawa T. Posterior reversible encephalopathy syndrome: a review with emphasis on neuroimaging characteristics. *J Neurol Sci* 2019;**404**:72–9.
33. Bartynski WS, Boardman JF. Distinct imaging patterns and lesion distribution in posterior reversible encephalopathy syndrome. *AJNR Am J Neuroradiol* 2007;**28**(7):1320–7.
34. Agarwal A, Kapur G, Altinok D. Childhood posterior reversible encephalopathy syndrome: magnetic resonance imaging findings with emphasis on increased leptomeningeal FLAIR signal. *Neuroradiol J* 2015;**28**(6):638–43.
35. Ejindu VC, Hine AL, Mashayekhi M, *et al*. Musculoskeletal manifestations of sickle cell disease. *RadioGraphics* 2007;**27**(4):1005–21.
36. Almeida A, Roberts I. Bone involvement in sickle cell disease. *Br J Haematol* 2005;**129**(4):482–90.
37. Saito N, Nadgir RN, Flower EN, *et al*. Clinical and radiologic manifestations of sickle cell disease in the head and neck. *RadioGraphics* 2010;**30**(4):1021–34.
38. Madani G, Papadopoulou AM, Holloway B, *et al*. The radiological manifestations of sickle cell disease. *Clin Radiol* 2007;**62**(6):528–38.
39. Watanabe M, Saito N, Nadgir RN, *et al*. Craniofacial bone infarcts in sickle cell disease. *J Comput Assist Tomogr* 2013;**37**(1):91–7.
40. Tuna IS, Tarhan B, Escobar M, *et al*. T2-blackout effect on DWI as a sign of early bone infarct and sequestration in a patient with sickle cell disease. *Clin Imaging* 2019;**54**:15–20.
41. Alqurashi MM, Raslan OM, Gmati GE. Spontaneous subgaleal hematoma in a sickle cell disease patient: a case report. *J Med Cases* 2020;**11**(2):46–8.
42. Berger E, Saunders N, Wang L, *et al*. Sickle cell disease in children. *Arch Paediatr Adolesc Med* 2009;**163**(3):251.
43. Umans H, Haramati N, Flusser G. The diagnostic role of gadolinium enhanced MRI in distinguishing between acute medullary bone infarct and osteomyelitis. *Magn Reson Imaging* 2000;**18**(3):255–62.